Int J Clin Exp Med 2023;16(11):275-282
www.ijcem.com /ISSN:1940-5901/IJCEM0150406

Original Article

Imaging diagnosis of malignant melanoma of nasal cavity and sinus and hemorrhage and necrotizing polyp of nasal cavity and sinus

Yuxiao He[1], Jing Zhang[1], Shuang Liu[1], Zhi Feng[2], Xiangguang Chen[2], Liang Jiang[1]

[1]Department of Otolaryngology, The Affiliated Hospital of Southwest Medical University, Luzhou 646000, Sichuan, China; [2]Radiographic, The Affiliated Hospital of Southwest Medical University, Luzhou 646000, Sichuan, China

Received March 28, 2023; Accepted October 15, 2023; Epub November 15, 2023; Published November 30, 2023

Abstract: The present study aimed to analyze the CT and MRI imaging findings in patients diagnosed with malignant melanoma of the nasal cavity and sinuses (SNMM) and necrotizing polyps (sinonasal organized hematoma, SOH). Nineteen patients with pathologically confirmed SOH and sixteen patients with pathologically confirmed SNMM were included in the analysis. The imaging characteristics assessed included the lesion's location on CT and MRI, as well as its margin and signal intensity (area of interest, ROI). The results revealed that the primary lesions of SNMM were found in 12 cases, while SOH was observed in 4 cases. Regarding relative CT values, no statistically significant differences were observed between SNMM and SOH ($P > 0.05$). Regarding MRI findings, five SNMM cases showed high signal intensity on T1-weighted imaging (T1WI) and low signal intensity on T2-weighted imaging (T2WI). In contrast, eight SOH cases mainly exhibited high signal intensity on T2WI. Statistical analysis revealed significant differences in relative T1 signal intensities within the regions of interest (ROI) ($P < 0.05$). Conversely, no statistically significant differences were found in the relative T2 signal intensities ($P > 0.05$). Moreover, through ROC curve analysis, the T1WI sequence in MRI demonstrated substantial diagnostic value in distinguishing SNMM from SOH. In conclusion, CT and MRI imaging techniques provide valuable information regarding the tumor site, surrounding bone destruction, and invasion of adjacent vital structures in patients with SNMM and SOH. Additionally, the T1WI sequence in MRI exhibits distinct characteristics that aid in diagnosing these conditions.

Keywords: Malignant melanoma of nasal cavity and paranasal sinus, hemorrhage and necrotizing polyp of nasal cavity and sinus, CT, MRI

Introduction

Malignant melanoma of the nasal cavity and sinuses (SNMM) is a malignant tumor in the head and neck region characterized by symptoms like nasal congestion and nasal hemorrhage, involving the nasal and sinus tissues [1]. This disease primarily affects middle-aged and elderly individuals over the age of 50, with no gender differences [2]. Hemorrhagic and necrotizing polyps of the nasal cavity and sinuses (SOH) are a distinct type of inflammatory polyps, also known as hemangiomatous or vasodilating polyps, accounting for only 4% to 5% of all nasal polyps [4]. The most commonly affected sinus is the maxillary sinus, although SOH can also occur in the nasal cavity, sphenoidal sinus, or frontal sinus [5]. SOH can develop at any age [6], and the common clinical symptoms, included nasal congestion and epistaxis [7, 8].

In the early stages, patients with SNMM do not exhibit specific manifestations, and most of them experience symptoms such as nasal congestion or bleeding. At this stage, the lesions tend to be larger, but they may not display typical imaging characteristics of melanoma [9]. On the other hand, the clinical manifestations of SOH do not significantly differ from the early clinical symptoms of SNMM, and distinguishing between the two solely based on visual inspection of the images is challenging. Therefore, it becomes crucial to differentiate them by comparing the signal intensity and value and con-

sidering the imaging characteristics of benign and malignant tumors.

Early detection, diagnosis, and treatment through imaging examinations improve patient outcomes and enhance survival time. Thus, MRI and CT imaging techniques are employed as diagnostic measures in clinical practice. This study investigated the diagnostic value and outcomes by applying these imaging modalities to diagnose 16 cases of malignant melanoma and 19 cases of hemorrhagic and necrotizing nasal polyps, as confirmed by surgical pathology in our hospital.

Data and methods

General information

Radiographic data from patients diagnosed with nasal and paranasal malignant melanoma and necrotizing polyps between July 2016 and March 2022 were included in the study. The dataset consisted of clinical data and CT or MRI imaging data from 16 patients with nasal and sinus malignant melanoma and 19 patients with hemorrhagic and necrotic nasal polyps. The data of these patients were accessible and obtained with the approval of the Clinical Trial Ethics Committee of the Affiliated Hospital of Southwest Medical University. The study adhered to the principles outlined in the Declaration of Helsinki. All procedures were conducted following the guidelines and regulations set forth by the ethics committee. Informed consent was obtained from all patients who participated in the study. **Table 1** provides a comprehensive overview of the clinical data collected.

The eligibility criteria for malignant melanoma of the nasal cavity and paranasal sinuses were as follows: ① Pathological confirmation of malignant melanoma in the nasal cavity and paranasal sinuses; ② Patients who had not undergone medication or surgery; ③ Patients who underwent CT or MRI examination. Ultimately, a total of 16 patients (10 males and 6 females) were included, resulting in a male-to-female ratio of approximately 5:3. The age of the patients ranged from 45 to 83 years, with an average age of 63.06 years. Regarding hemorrhage and necrotizing polyps of the nasal cavity and sinuses, the inclusion criteria were: ① Patients with pathologically confirmed nasal and sinonasal hemorrhage; ② Patients who had not undergone medication or surgery; ③ Patients who underwent CT or MRI examination, with symptoms, physical examination, and examination predominantly affecting one side. In total, 19 patients (14 males and 5 females) were enrolled, resulting in a male-to-female ratio of approximately 14:5. The age of the patients ranged from 28 to 71 years, with an average age of 49.18 years. The following were the exclusion criteria: ① Patients diagnosed with SNMM and SOH without pathological confirmation; ② Patients who had undergone medical or surgical treatment; ③ Patients who had not undergone CT or MRI examination; Symptoms, physical examination, and examination affecting both sides.

CT and MRI examination methods

CT examination method: Sinus CT scans were performed using a 256-row spiral CT scanner, with scanning from the top of the frontal sinus to the level of the maxillary sinus floor. The patients were positioned in the supine position with their jaw raised, maintaining calm breathing throughout the scan. They were instructed not to swallow during the procedure, and trained to hold their breath before the examination. The scanning plane was parallel to the hyoid bone, covering the area from the hyoid to the thyroid level. The scan parameters were set as follows: 120 kV, 200 mA, 2 mm slice thickness, 2 mm interslice distance, a FOV of 30 cm, and a matrix size of 512 × 512. Soft tissue and bone windows were utilized to assess soft tissue lesions and surrounding bone structures. An iodine contrast agent was injected through the cubital vein at a rate of 3.5 mL/s for contrast enhancement.

MRI examination method: A Philips 1.5T MR scanner equipped with a 16-channel neck phased array surface coil was utilized. The scanning protocol included T1WI and T2WI with TSE sequences. The scanning parameters were as follows: (1) T1WI-TSE sequence: TR = 457.48 ms, TE = 5.13 ms, matrix size of 186 × 244, 5.5 mm slice thickness, 1 mm interslice interval, and a FOV of 22.1 cm × 22.1 cm. (2) T2WI-TSE sequence: TR = 4000 ms, TE = 80 ms, matrix size of 183 × 244, 5 mm slice thickness, 1 mm interslice interval, and a FOV of 22.1 cm × 22.1 cm. Gadolinium-based contrast agent was

Table 1. Patient clinical data sheet

	Number of cases of malignant nasal cavity and paranasal sinus melanoma n (100%)	Nasal and paranasal sinus hemorrhage necrotizing polyps Number of cases in the n (100%)
Sex		
Man	10 (62.5%)	14 (73.68%)
Woman	6 (37.5%)	5 (26.32%)
Age		
< 40	0 (0.00%)	3 (15.79%)
41-50	3 (18.75%)	9 (47.37%)
51-60	4 (25%)	5 (26.32%)
61-70	6 (37.5%)	1 (5.26%)
> 70	3 (18.75%)	1 (5.26%)
The primary site of the lesion		
Nasal cavity	12 (75%)	4 (21.05%)
Antrum highmori	3 (18.75%)	13 (68.42%)
Antrum ethmoidale	0 (0%)	3 (15.79%)
Frontal sinuses	0 (0%)	0 (0%)
Sphenoid sinus	1 (6.25%)	0 (0%)
Clinlcal symptom		
Hemorrhinia	16 (100%)	12 (63.16%)
Rhinobyon	14 (87.5%)	16 (84.21%)
Hyposmia	7 (43.75%)	8 (42.11%)
Nasal new creatures	16 (100%)	11 (57.89%)
Maxillofacial pain	5 (31.25%)	1 (5.26%)
Dry eyes, overflowing tears, and blurred vision	5 (31.25%)	4 (21.05%)
Headache	3 (18.75%)	8 (42.11%)
Osteopathic changes		
Expansion growth	13 (81.25%)	15 (78.94%)
Invasive growth	3 (23.07%)	4 (21.05%)
Therapy method		
Surgical operation	8 (50%)	19 (100%)
Radiotherapy chemotherapy	2 (12.5%)	0 (0%)
Surgery + Radiotherapy/chemotherapy	6 (37.5%)	0 (0%)

administered for enhanced scanning, with a dosage of 0.1 mmol/kg.

Image analysis

Two expert radiologists specializing in head and neck imaging thoroughly examined all CT and MRI images and achieved a consensus. The analysis focused on the imaging characteristics observed on CT scans, including the shape, location, expansibility, and CT values. Similarly, the analysis encompassed the imaging features observed on MRI scans, including the shape, location, expansibility, and signal intensity.

Data processing

Signal measurements were conducted for SNMM and SOH, focusing on the T1WI sequence. In the case of SNMM, three ROI were placed within the abnormal signal region, as well as in the adjacent lingual body region with normal signal intensity. The average signal value for each ROI was calculated. Additionally, the maximum level region of interest (ROI) within the solid part of the lesion was selected. The ROI area should be greater than 2/3 of the lesion cross-section for uniformly dense lesions. In the case of heterogeneous density, the region with the most genuine components

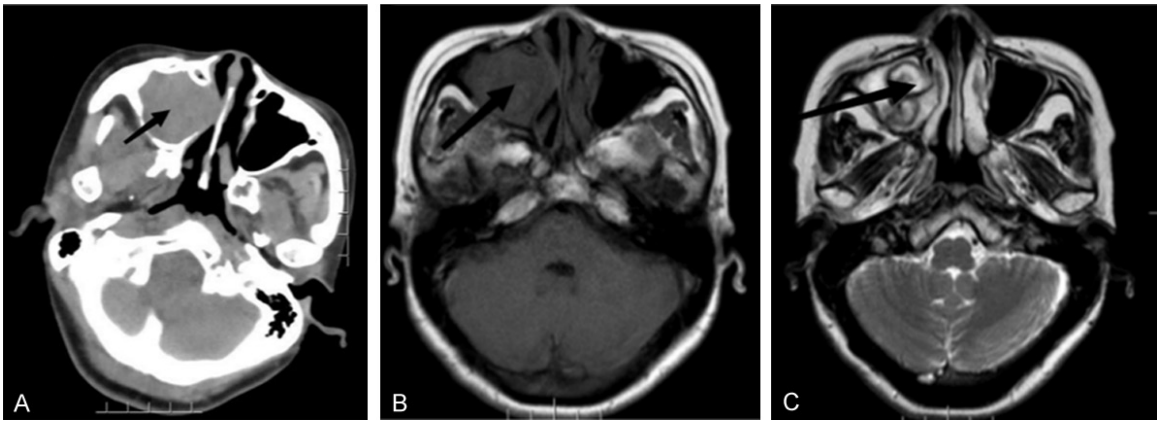

Figure 1. The patient in this case was a 55-year-old male. The postoperative pathological diagnosis confirmed hemorrhage and necrotizing polyp of the nasal cavity and sinus. (A) A soft tissue shadow is observed in the right sinus, filling the sinus cavity with uneven density and enhancement. (B, C) Irregular nodules and a distinct mass shadow with clear boundaries are visible. But On (C) T1-weighted imaging (T1WI), the signal is predominantly high.

in the hierarchical structure was chosen for measurement. The relative T1 signal value was determined by dividing the mean signal value of SNMM by the mean signal value of the adjacent lingual body. The same method was applied to obtain the relative T2 signal values and relative CT values for both SNMM and SOH. The ROI of SNMM and SOH ranged from 25 mm^2 to 30 mm^2.

Statistical method

Statistical analysis was performed using SPSS 26.0 software. Measurement data were assessed for normal distribution and expressed as mean ± SD. To compare measurement data between groups, the independent sample t-test was utilized. A *p*-value less than 0.05 was considered statistically significant. The sensitivity, specificity, accuracy, positive predictive value, negative predictive value, and area under the ROC curve (AUC) were calculated to analyze the diagnostic performance, using the ROC curve analysis.

Results

Patient clinical data results and imaging findings

The primary sites of SNMM and SOH in the nasal cavity were observed in 12 and 4 cases, respectively. In terms of sinus involvement, SNMM was found in 3 cases in the maxillary sinus and 13 cases in the ethmoid sinus, while SOH was detected in 0 cases in the ethmoid sinus and 3 cases in the sphenoid sinus. No cases were identified in the frontal sinus. SNMM exhibited irregular focal morphology with expansive growth, whereas SOH displayed lobulated and massive lesion shapes, mostly characterized by expansive growth (**Figures 1**, **2**). Locally infiltrative margins were observed in three cases of SNMM and four cases of SOH.

Comparison of statistical parameters of CT values and relative signal values of each MRI sequence

On CT, there was no statistically significant difference in the relative CT values between the two groups ($P > 0.05$) (**Table 2**). On MRI, five cases of SNMM demonstrated high signal intensity on T1WI and low signal intensity on T2WI. The remaining 11 cases exhibited various MRI characteristics, including low signal on T1WI, high signal on T2WI, and mixed signals on both T1WI and T2WI (**Figure 2B**, **2C**). Conversely, eight cases of SOH predominantly presented with high signal intensity on the T2WI sequence. Intralesional enhancement scans of SNMM and SOH showed heterogeneous and significantly enhanced patterns. Statistical analysis revealed a statistically significant difference in the relative T1 signal values between the two ROI ($P < 0.05$) (**Table 2**). However, there was no significant difference in the relative T2 signal values ($P > 0.05$) (**Table 2**).

ROC curve analysis

Figure 3 demonstrates that the T1WI sequence in MRI had a significant discriminatory value for

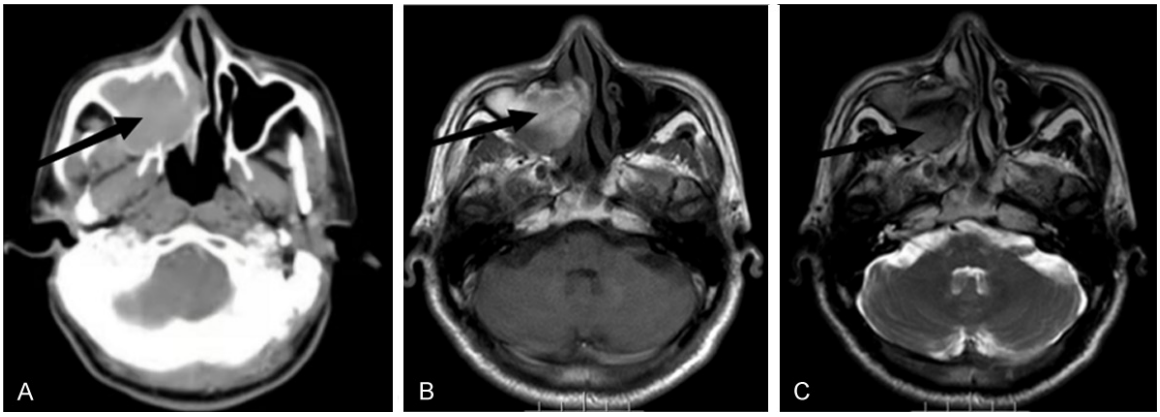

Figure 2. The patient in this case was a 48-year-old female. The postoperative pathological diagnosis confirmed malignant melanoma of the nasal cavity and paranasal sinus. A. Depicts the right maxillary sinus appears enlarged, displaying uneven moderate enhancement in the area of low density. B. A slightly higher mixed signal intensity on T2-weighted imaging (T2WI). C. The right maxillary sinus exhibits a mixed high signal intensity on T1-weighted imaging (T1WI).

Table 2. Relative CT values and statistical parameters of relative signal values of each MRI sequence (Mean ± SD)

Target	SOH	SNMM	*t*	*P*
Relative CT values	1.21±0.41	1.55±0.39	-2.015	0.058
Relative T1 signal values	0.81±0.15	1.02±0.25	-2.427	0.025
Relative T2 signal values	1.56±0.47	1.39±0.41	0.897	0.380

The independent sample t-test showed the relative T1 signal difference between the two groups ($P < 0.05$); the relative CT value and relative T2 signal value were not different between the two groups ($P > 0.05$).

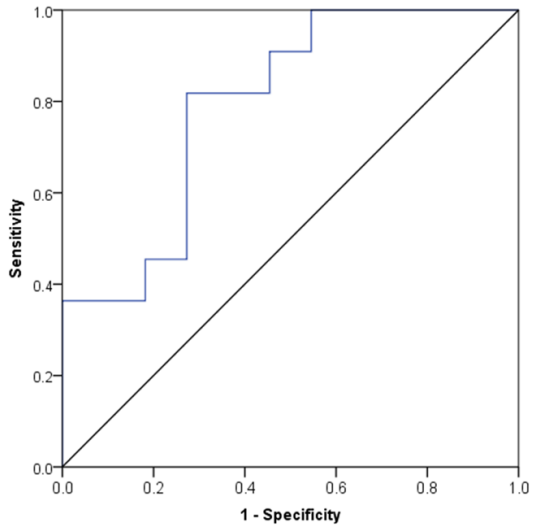

Figure 3. ROC plot of the relative T1 signal values between SNMM and SOH.

distinguishing malignant melanoma of the nasal cavity and sinuses from necrotizing polyps of the nasal cavity and sinus hemorrhage. The area under the curve (AUC) was 0.793. AUC varies from 0.5 (no apparent accuracy) to 1.0 (perfect accuracy) as the ROC curve moves towards the left and top boundaries of the ROC graph [10]. The diagnostic performance for malignant melanoma of the nasal cavity and sinuses and necrotizing polyps of the nasal cavity and sinus hemorrhage was as follows: sensitivity of 81.82%, specificity of 72.73%, accuracy of 68.18%, positive predictive value of 75.00%, and negative predictive value of 80.00% (**Table 3**).

Discussion

Malignant melanoma is a highly malignant form of skin cancer characterized by its potential for early metastasis and high mortality rate. Although rare in clinical practice, malignant melanoma of the nasal cavity and sinuses has shown a significant increase in incidence in recent years. Diagnosis of this condition can be challenging, as many patients may not display obvious symptoms and fail to receive timely clinical assessment and examination, leading to diagnostic delays [11]. Given the rapid progression and significant impact of malignant melanoma on patients, improving the accuracy of diagnostic outcomes is crucial to facilitate timely detection and provide a solid foundation for effective surgical interventions [12]. When assessing cases of hemorrhagic and necrotizing nasal polyps through imaging, the presence

Table 3. Diagnostic efficacy of relative T1 signal values in differentiating SNMM and SOH

Target	Sensitivity	Specificity	Accuracy	Positive predictive value	Negative predictive value	AUC
Relative T1 signal values	81.82%	72.73%	68.18%	75.00%	80.00%	0.793

of a hematoma can sometimes be mistaken for a malignant lesion. Clinical manifestations, such as epistaxis, cheek swelling, proptosis, and oral mass, may resemble malignancy [13]. In this context, imaging examinations play a critical role in the accurate clinical diagnosis of tumors. Both MRI and CT scans are employed in the clinical diagnosis of necrotizing polyps and malignant melanoma of the nasal cavity and sinuses. Since distinguishing between SNMM and SOH solely through visual examination is challenging, these imaging modalities provide valuable information regarding the location of the lesion, the extent of bone or surrounding tissue invasion, and changes in signal intensity. This enables the formulation of reliable treatment plans and improves the overall efficacy of surgical interventions.

Table 1 provides an overview of the clinical manifestations and imaging data for 16 cases of malignant melanoma of the nasal cavity and sinuses and 19 cases of necrotizing polyps with the nasal cavity and sinus hemorrhage. The average age at diagnosis for the SNMM patients was 63.06 years, predominantly affecting elderly individuals with no notable gender difference. The nasal mucosa was the primary site of onset, consistent with previous literature reports [3]. In the case of necrotizing polyps with nasal and sinus hemorrhage, the average age at diagnosis was 49.18 years, mainly affecting younger individuals, and the maxillary sinus mucosa was the primary site of onset, consistent with previous literature findings [14]. A Swedish study conducted using the NCDB reported a significant increase in the incidence of SNMM, particularly among females. The study spanned 41 years, and the incidence among men increased at an even faster rate. It also highlighted a higher incidence with advancing age, peaking after the age of 80 [15]. CT imaging allows visualization of the mass morphology, adjacent bone destruction, and the extent of surrounding tissue invasion in malignant melanoma of the nasal cavity and paranasal sinuses [16]. As illustrated in **Figure 2A**, the CT image reveals an irregular soft tissue mass in the right maxillary sinus, along with thin bone absorption in the right turbinate and the inner and outer walls of the maxillary sinus. The right maxillary sinus appears enlarged, and the enhanced scans demonstrate heterogeneous and moderate enhancement. Malignant melanoma of the nasal cavity and paranasal sinuses exhibits certain characteristics on MRI images. Typically, melanoma appears as a high signal intensity in T1WI and a low signal intensity in T2WI [17]. The findings of this study indicate that out of the thirteen SNMM patients, irregular soft tissue density shadows were observed, indicating swelling growth without apparent cysts or calcification. All adjacent bones displayed osteolytic changes, and all tumors showed invasion of the surrounding tissues. The primary sites of onset were located in the nasal mucosa in twelve cases, the maxillary sinus in three cases, and the sphenoidal sinus in one case. Five cases exhibited high signal intensity in T1WI and low signal intensity in T2WI, while the remaining eleven cases displayed various MRI characteristics, including low signal intensity in T1WI, high signal intensity in T2WI, mixed signals in both T1WI and T2WI (as shown in **Figure 2B**, **2C**). These results also reflect the high sensitivity of MRI to melanin. Electrons from free radicals in melanin interact with free water, resulting in a shortening of T1 and a relative shortening of T2. Therefore, the shortened T1 values correspond to neuropathological findings of melanocytic deposits or melanocytic tumors. T2WI exhibited a hypointense mass shadow, which is also a characteristic feature of melanocytomas [18]. In CT, the heterogeneous density of nasal polyps is determined by the pathological changes associated with bleeding and necrosis [19, 20]. Enhanced scans often reveal lesions with heterogeneous enhancement. Although CT imaging does not provide characteristic findings for hemorrhagic and necrotizing nasal polyps, it offers a more intuitive visualization of changes in the adjacent bone structure compared to MRI [21, 22]. In this study, the lesions observed in SOH patients exhibited mixed soft tissue density masses with areas of high and low den-

sity. Specifically, 13 lesions were located in the maxillary sinus mucosa, 4 in the nasal mucosa, and 3 in the ethmoid sinus mucosa. These lesions displayed uneven enhancement (**Figure 1A**). Maxillary sinus enlargement and compression-resorption destruction of the adjacent maxillary sinus wall were also evident. MRI imaging effectively demonstrated the location and morphological outline of the lesions in SOH patients. The typical characteristic was the growth of the adjacent maxillary sinus, with some lesions protruding into the middle nasal passage [23]. Additionally, in T2WI, the lesions exhibited mixed high and low signal intensities, often surrounded by a low signal intensity ring [24]. Studies have suggested that this hypointensity corresponds to hemosiderin deposition resulting from pedicle torsion of nasal polyps or extrusion of the maxillary sinus, leading to tortuous vessel rupture and old bleeding [25]. Among the SOH patients in this study, 8 exhibited predominantly high signal intensity on the T2WI sequence (**Figure 1B**, **1C**). The right maxillary sinus showed cavity enlargement with irregular nodules and mass shadows, partial fusion, and clear boundaries. T2WI demonstrated a predominance of high signal intensity, and the enhancement scans within the lesion displayed heterogeneous and significantly enhanced patterns. The relative T1 signal values derived from the T1WI sequence in this study proved to be of great value in differentiating between SNMM and SOH. Statistical analysis of the signal values within the region of interest (ROI) demonstrated significant differences in relative T1 signal values between SNMM and SOH ($P < 0.05$), as shown in **Table 2**. Using ROC curve analysis (**Figure 3**), the T1WI sequence achieved sensitivity, specificity, and accuracy rates of 81.82%, 72.73%, and 68.18% (**Table 3**), respectively, in distinguishing between SNMM and SOH. However, this study also has certain limitations. Firstly, it lacks pathological classification between the two conditions. Secondly, the cases examined were relatively rare. Future research should aim to address these limitations in greater detail.

Conclusion

CT and MRI imaging modalities offer valuable insights into the localization of SNMM and SOH masses, as well as the assessment of surrounding bone destruction and invasion into adjacent critical structures. While they provide some useful information for clinical evaluation, CT imaging lacks distinct characteristics for SNMM and has limitations in achieving a definitive diagnosis. In contrast, the signal intensity and size of the mass on T1WI sequences in MRI play a crucial role in distinguishing between SNMM and SOH.

Disclosure of conflict of interest

None.

Address correspondence to: Dr. Liang Jiang, Department of Otolaryngology, The Affiliated Hospital of Southwest Medical University, Luzhou 646000, Sichuan, China. Tel: +86-08303165641; E-mail: jiangliang56821015@swmu.edu.cn

References

[1] Vazquez A, Khan MN, Blake DM, Patel TD, Baredes S and Eloy JA. Sinonasal squamous cell carcinoma and the prognostic implications of its histologic variants: a population-based study. Int Forum Allergy Rhinol 2015; 5: 85-91.

[2] Pincet L, Lambercy K, Pasche P, Broome M, Latifyan S and Reinhard A. Mucosal melanoma of the head and neck: a retrospective review and current opinion. Front Surg 2021; 7: 616174.

[3] Sheahan P, Crotty PL, Hamilton S, Colreavy M and McShane D. Infarcted angiomatous nasal polyps. Eur Arch Otorhinolaryngol 2005; 262: 225-230.

[4] Yfantis HG, Drachenberg CB, Gray W and Papadimitriou JC. Angiectatic nasal polyps that clinically simulate a malignant process: report of 2 cases and review of the literature. Arch Pathol Lab Med 2000; 124: 406-410.

[5] Park SY and Kim KS. Giant organized hematoma originating from the inferior turbinate. Iran J Radiol 2015; 12: e12366.

[6] De Vuysere S, Hermans R and Marchal G. Sinochoanal polyp and its variant, the angiomatous polyp: MRI findings. Eur Radiol 2001; 11: 55-58.

[7] Kim EY, Kim HJ, Chung SK, Dhong HJ, Kim HY, Yim YJ, Kim ST, Jeon P and Ko YH. Sinonasal organized hematoma: CT and MR imaging findings. AJNR Am J Neuroradiol 2008; 29: 1204-1208.

[8] Song HM, Jang YJ, Chung YS and Lee BJ. Organizing hematoma of the maxillary sinus. Otolaryngol Head Neck Surg 2007; 136: 616-620.

[9] Han WT. Clinical imaging analysis of 130 cases of nasal and sinus tumors. China Pract Med 2015; 10: 66-67.

[10] Hanley JA and McNeil BJ. The meaning and use of the area under a receiver operating characteristic (ROC) curve. Radiology 1982; 143: 29-36.
[11] Chen HY, Liu L, Tian ZB, Jin YD and Jin RS. Clinicopathological features and literature review of primary malignant melanoma of nasal cavity and sinuses. Exp Labor Med 2018; 36: 117-119.
[12] Jiang AH. Analysis of diagnosis by fine needle aspiration biopsy for 1 cases of patient with primary malignant melanoma. Contemp Med Symp 2017; 15: 33-34.
[13] Yagisawa M, Ishitoya J and Tsukuda M. Hematoma-like mass of the maxillary sinus. Acta Otolaryngol 2006; 126: 277-281.
[14] Omura G, Watanabe K, Fujishiro Y, Ebihara Y, Nakao K and Asakage T. Organized hematoma in the paranasal sinus and nasal cavity--imaging diagnosis and pathological findings. Auris Nasus Larynx 2010; 37: 173-177.
[15] Jangard M, Hansson J and Ragnarsson-Olding B. Primary sinonasal malignant melanoma: a nationwide study of the Swedish population, 1960-2000. Rhinology 2013; 51: 22-30.
[16] Wang Y, Guan B, Xu L, Xu Y and Zhang J. Clinical analysis of 23 cases of malignant melanoma of nasal cavity and sinuses. J Clin Otolaryngol Head Neck Surg 2014; 28: 1559-1561.
[17] Wang M, Li H and Ma S. Advances in clinical diagnosis and treatment of sinonasal mucosal malignant melanoma. J Otolaryngol Ophthalmol Shandong Univ 2017; 31: 116-120.
[18] Huang HY, Huang WH, Shu JE and Wang F. Diagnostic value of 3T MRI in malignant melanoma and squamous cell carcinoma of nasal cavity and sinuses. Mod Pract Med 2017; 29: 525-527.
[19] Zou J, Man F, Deng K, Zheng Y, Hao D and Xu W. CT and MR imaging findings of sinonasal angiomatous polyps. Eur J Radiol 2014; 83: 545-551.
[20] Wu J and Lu Z. The diagnostic value of CT in hemorrhagic and necrotic polyps of maxillary sinus and nasalcavity. J Pract Radiol 2004: 18-20.
[21] Lou H, Meng Y, Piao Y, Wang C, Zhang L and Bachert C. Predictive significance of tissue eosinophilia for nasal polyp recurrence in the Chinese population. Am J Rhinol Allergy 2015; 29: 350-356.
[22] Xu XM and Dang XH. Endoscopic surgery and clinical analysis of hemorrhagic necrotic nasal polyp. Chin J Otorhinolar-Skull Base Surg 2007; 13: 126-128.
[23] Wang YZ, Yang BT, Wang ZC, Song L and Xian JF. MR evaluation of sinonasal angiomatous polyp. AJNR Am J Neuroradiol 2012; 33: 767-772.
[24] Li P, Liu Y, Hou WH, Zhang JS and Huan Y. MRI in diagnosis of hemorrhagic and necrotic nasal polyps. Chin J Med Imag Technol 2015; 31: 37-40.
[25] Nishiguchi T, Nakamura A, Mochizuki K, Tokuhara Y, Yamane H and Inoue Y. Expansile organized maxillary sinus hematoma: MR and CT findings and review of literature. AJNR Am J Neuroradiol 2007; 28: 1375-1377.